Conformational Space and Photochemistry of α-Terpinene

K. M. Marzec,[†] I. Reva,[‡] R. Fausto,*[,‡] K. Malek,[†] and L. M. Proniewicz*[,†]

Faculty of Chemistry, Jagiellonian University, Ingardena 3, 30-060 Krakow, Poland, and Departament of Chemistry, University of Coimbra, P-3004-535 Coimbra, Portugal

Received: January 26, 2010; Revised Manuscript Received: March 23, 2010

α-Terpinene is a natural product that is isolated from a variety of plant sources and is used in the pharmaceutical and perfume industries. In the atmosphere, under the influence of sunlight, α-terpinene undergoes a series of photochemical transformations and contributes to the formation of the secondary organic aerosols. In the present work, α-terpinene has been isolated in low-temperature xenon and argon matrices, and its structure and photochemistry were characterized with the aid of FTIR spectroscopy and DFT calculations. The theory predicts three conformers resulting from the rotation of the exocyclic $CH(CH_3)_2$ framework, that is, Trans (T) and Gauche (G+ and G−) forms. The two Gauche conformers were estimated to be higher in energy, by ca. 1.75 kJ mol^{-1}, than the most stable Trans form. The signatures of all three conformers were found to be present in the experimental low-temperature matrix spectra with the T form dominating in diluted matrices. The conformational ratio was found to shift in favor of the G+/G− forms upon annealing of the matrices as well as in the neat α-terpinene liquid. UV−C (λ > 235 nm) irradiation of matrix-isolated α-terpinene led to its isomerization into an open-ring species, which is produced in the Z configuration and in the conformations that require the smallest structural rearrangements of both the reagent and matrix.

Introduction

α-Terpinene (1-isopropyl-4-methyl-1,3-cyclohexadiene) belongs to the group of monocyclic terpinenes, commonly designated as monoterpenes. The growing interest for this compound is mainly related to its bioactivity as an antibacterial, antifungal, anti-inflammatory, anticancer, and antioxidant agent, which justifies its pharmacological uses.[1,2] Because of its pleasant odor, α-terpinene has also been used as a fragrance ingredient in cosmetics and food industries.[3,4]

Until now, most of the studies on monoterpenes have been focused on their identification and quantitative analysis in plants. These analyses have been carried out by using physicochemical methods such as gas chromatography−mass spectrometry (GC-MS),[5,6] gas chromatography−pyrolysis−isotope ratio mass spectrometry,[7] nuclear magnetic resonance (NMR),[8,9] and vibrational spectroscopy.[9−11] However, α-terpinene has not been studied extensively as a topic compound.[4]

The photochemical behavior of terpenes has been investigated to shed light on decomposition processes that might be relevant for their above-mentioned applications.[12,13] It was found that the UV irradiation of essential plant oils such as the oils of the tea tree or lemon, under aerobic and warm conditions, leads to photochemical changes in their constituting monoterpenoids. These studies have shown that under conditions mimicking the natural atmospheric conditions, an increase in the concentration of *p*-cymene occurs with simultaneous lowering of the amount of other monoterpenoids, such as α-terpinene, γ-terpinene, terpinolene, and limonene.[13−15] These results suggest that the deterioration process of food products containing α-terpinene occurs through the sterically favored photo-oxidation mechanism that leads to conversion of α-terpinene mainly into *p*-cymene.[16]

SCHEME 1: Experimentally Observed Photochemistry of α-Pyrone (Top),[24] 1,3-Cyclohexadiene (CHD, Middle),[30−32] and the Possible Analogous Photoreactions of α-Terpinene (Bottom)

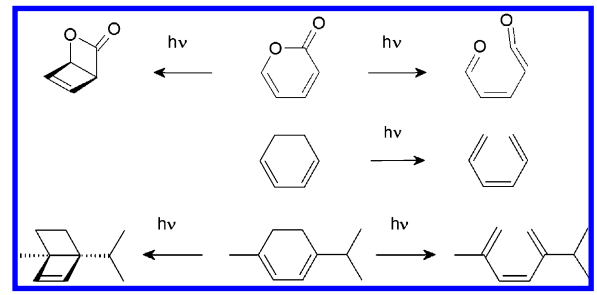

In the presence of oxygen, other photoproducts of α-terpinene have also been reported, such as ascaridol, isoascaridol, and ketoperoxide.[17,18]

For several groups of six-membered unsaturated ring compounds, the general preferred photochemical reactions have been shown to be the ring-opening and ring-contraction reactions.[19−23] The first type of photoreaction generates the isomeric open ring compounds, whereas the second type results in the rearrangement of the ring and formation of Dewar-like isomers. The prototype system is α-pyrone, whose photochemistry has deserved much attention since long ago and has recently been studied in detail in our laboratory.[24] α-Pyrone and α-terpinene show a common *cis*-1,3-diene fragment inserted in a six-membered ring, and we can expect some similarities in their photochemistries (Scheme 1). The photochemistry of α-terpinene's parent molecule, 1,3-cyclohexadiene (CHD), was also previously investigated by several theoretical and experimental methods, such as semiclassical dynamics simulation, time-resolved UV resonance Raman and nanosecond time-resolved step-scan FTIR spectroscopies, multiphoton ionization and others.[21,25−29] It has been found that CHD undergoes the ring-

* Corresponding authors. (L.M.P.) E-mail: proniewi@chemia.uj.edu.pl. Tel: +48 12 663 2288. (R.F.) E-mail: rfausto@ci.uc.pt. Tel: +351 91 9236971.
[†] Jagiellonian University.
[‡] University of Coimbra.

10.1021/jp100770v
Published on Web 04/13/2010

opening photoreaction,[30−32] and no other photoproducts have been reported so far.

Up to now, the photochemical reactions of α-terpinene have been studied by ab initio multistate second-order perturbation theory and gas-phase UV spectroscopy.[29] The latter has revealed that α-terpinene, similarly to CHD, may undergo the ring-opening conversion. However, to the best of our knowledge, this hypothesis has not yet been confirmed by other studies.

In the present work, we report an investigation of the structure, spectroscopy, and photochemistry of matrix-isolated α-terpinene. Monomers of α-terpinene were isolated in low-temperature argon and xenon matrices and then submitted to in situ UV irradiation. In addition, liquid α-terpinene at room temperature was also investigated by FTIR-ATR and FT-Raman spectroscopies. Differences in the conformational preferences of α-terpinene in the gas and the condensed phase were observed. The experimental studies were complemented by quantum chemical calculations. On the basis of these studies, we discuss the conformational space of the molecule and the barriers of interconversion between its conformers. The calculations were also employed in the identification of the spectroscopically observed photoproducts. Finally, we present a vibrational assignment of the spectra carried out with the help of normal coordinate analysis calculations.

Experimental and Computational Methods

α-Terpinene was provided by Fluka (purum, ≥95.0% (GC)). The matrix gases, argon N60 and xenon N45, were supplied by Air Liquide.

The low-temperature equipment was based on an APD Cryogenics closed-cycle helium refrigerator with a DE-202A expander. For preparation of diluted matrices of the compound, α-terpinene and xenon were premixed manometrically in a molar ratio of about 1:500. For concentrated matrices, α-terpinene was deposited from a Knudsen cell through a needle valve. The valve nozzle was kept at room temperature, which defined the conformational distribution in the gas phase prior to deposition. The host matrix gas was deposited from a separate inlet. Temperature of the cold CsI window of the cryostat was kept at 10 (argon matrices) and 20−30 K (xenon matrices) and was measured directly at the sample holder by a silicon diode temperature sensor connected to a digital temperature controller (Scientific Instruments, model 9650-1), which provides an accuracy of 0.1 K. The matrix isolation IR spectra were collected on a Nicolet 6700 Fourier transform infrared spectrometer equipped with a deuterated triglycine sulfate (DTGS) detector and a Ge/KBr beam splitter with 0.5 cm^{-1} spectral resolution. Other details of the matrix isolation experimental setup can be found elsewhere.[33]

The matrices were irradiated using a 200 W output power of a 300 W Hg/Xe lamp (Oriel, Newport) and a series of long-pass optical filters through the quartz or KBr (λ > 235 nm) external windows of the cryostat.

The spectrum (650−4000 cm^{-1}) of the liquid compound (ca. 5−10 μL sample placed on the surface of a diamond-ZnSe ATR crystal with 0.5 mm diameter) was recorded using a portable diamond "TravelIR" spectrometer fitted with a deuterated L-alanine-doped triglycine sulfate (DLATGS) detector in a single reflection configuration. Sixteen scans with a spectral resolution of 4 cm^{-1} were accumulated.

The Raman spectrum of the liquid compound was recorded at room temperature on a Nicolet NXR 9650 FT-Raman spectrometer equipped with a Nd/YAG laser emitting at 1064 nm (9398.5 cm^{-1}) and a germanium detector cooled with liquid nitrogen. The power of the laser at the sample position was 100 mW. We collected and averaged 512 scans with a resolution of 4 cm^{-1}.

Density functional theory (DFT) calculations were carried out using the Gaussian 03 program package.[34] The geometries of the possible conformers of α-terpinene as well as those of its photoproducts were fully optimized at the B3LYP/6-311++G(d,p) level of theory.[35] To assess the effect of the applied method on relative energies of the conformers, we also conducted computations at the B3LYP/6-311++G(3df,3pd) and MP2/6-311++G(d,p) levels of approximation. Additionally, we modeled the possible interactions between the molecule and argon matrices by using the polarizable continuum model (PCM) at the B3LYP/6-311++G(d,p) level of theory.[36,37]

Theoretical Raman intensities I_i^R were obtained from the Gaussian 03 calculated Raman scattering activities (S_i) according to the expression[38] $I_i^R = 10^{-12}(\nu_0 - \nu_i)^4 \nu_i^{-1} S_i$, where ν_0 is the excitation wavenumber and ν_i is the calculated wavenumber of the normal mode i. Prior to comparison of the calculated wavenumbers with the experimental counterparts (IR and Raman spectra), the latter were scaled down by appropriate scale factors (0.978 and 0.960 for the 0−2000 and 2000−4000 cm^{-1} regions, respectively[39]), mainly to account for anharmonicity effects, basis set truncation, and the neglected part of electron correlation. A set of internal coordinates defined as suggested by Pulay, Fogarasi and co-authors[40,41] was used in normal coordinate analysis calculations[42] to assist in the assignment of the calculated IR and Raman spectra.

Results and Discussion

Conformational Equilibrium of α-Terpinene in the Gas Phase. α-Terpinene is characterized by one conformationally relevant internal rotation axis, which corresponds to the rotation of the isopropyl group. The present B3LYP calculations led to the identification of three minima on the molecule's potential energy surface, corresponding to conformers Trans, Gauche+, and Gauche− (Figure 1), all of them belonging to the C_1 symmetry point group. The conformers are named here according to the orientation of the $C_6-C_2-C_4-H_{25}$ dihedral angle. The optimized geometries of these conformers are given in Table S1 (Supporting Information), whereas the values of relative energies and dipole moments are presented in Table 1.

The conformational ground state corresponds to conformer Trans (T). The two gauche conformers (G+/G−) are calculated to be 1.76 and 1.75 kJ mol^{-1} higher in energy, respectively, than the Trans form (zero-point-corrected energies). Because of the small energy differences, all forms are expected to be significantly populated in the gas phase.

The potential energy profile for interconversion between the three conformers (Figure 2) shows that the barriers for T → G+, G+ → G−, and T → G− isomerizations are 15, 6, and 17 kJ mol^{-1}, respectively. The relatively high barriers between the Trans and Gauche forms can be expected to preclude interconversion between these conformers during their landing and cooling on the surface of the optical substrate in the process of deposition of the matrices. This implies that the relative populations of the isomers of α-terpinene trapped in the Ar and Xe matrices should be the same as those in the gas phase prior to deposition. Because the matrices presented here were obtained from α-terpinene vapor at room temperature, the conformational composition of the samples should then reflect the conformational equilibrium in the gas phase at that temperature. According to the Boltzmann statistics, the G+/G−/T population ratio estimated from the calculated Gibbs free energies at 298 K (2.18,

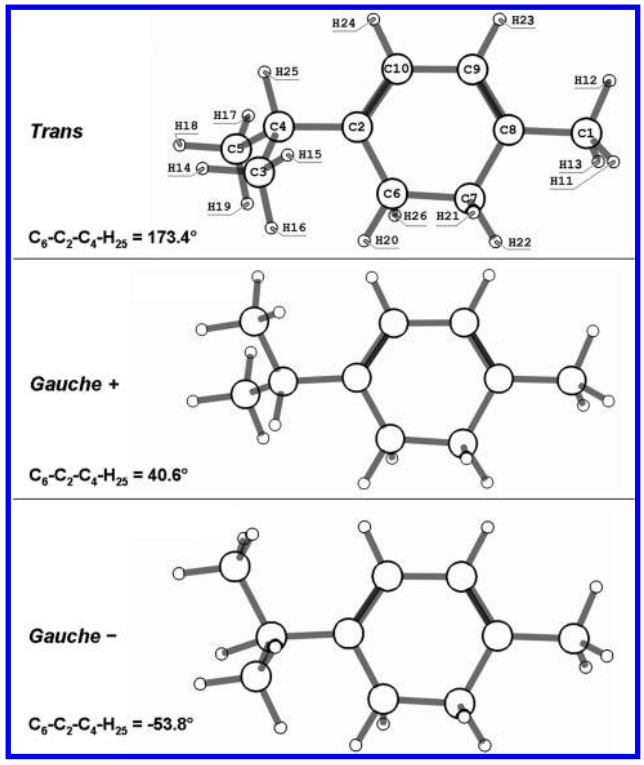

Figure 1. Conformers of α-terpinene with atom numbering. The conformers are named here according to the value of the $C_6-C_2-C_4-H_{25}$ dihedral angle, defining the orientation of the isopropyl group in relation to the ring.

TABLE 1: DFT(B3LYP)/6-311++G(d,p) Calculated Relative Energies without (ΔE°) and with (ΔE°_{ZPVE}) Zero-Point Corrections, Relative Gibbs Energies (ΔG°), and Dipole Moments ($|\mu|$) of α-Terpinene Conformers[a]

conformer	ΔE°	ΔE°_{ZPVE}	ΔG°	$\|\mu\|$
trans (T)	0.00	0.00	0.00	0.54
gauche (G+)	1.34	1.76	2.18	0.63
gauche (G−)	1.41	1.75	2.25	0.65

[a] Calculated energies of the closed-ring Trans conformer of α-terpinene were chosen as the zero level. The relative calculated energies of the remaining forms are given in kilojoules per mole. The corresponding absolute energies of the T conformer (all in hartree) are: electronic energy, $\Delta E^\circ = -390.790963646$; zero-point vibrational energy corrected, $\Delta E^\circ_{ZPVE} = -390.557515$; and Gibbs free energy (at 298.15 K), $\Delta G^\circ = -390.593503$. Dipole moments ($|\mu|$/debye).

2.25, 0 kJ mol^{-1}, respectively) is 0.228:0.222:0.550 (i.e., ∼1:1:2.5). Therefore, we simulated the IR spectrum representing this conformational distribution by adding the B3LYP calculated spectra of the individual conformers, with intensity scale factors proportional to their estimated population. This theoretical spectrum is compared with the experimental spectra of α-terpinene isolated in argon and xenon matrices in Figure 3.

Although the calculated spectra for the two Gauche conformers are very similar, the agreement between the experimentally observed spectrum and the spectrum simulated as described above confirmed the presence in the matrices of the three conformers of α-terpinene predicted theoretically and also the reliability of the calculations in predicting their relative energies. In addition, it facilitated the detailed assignment of the spectra (Tables S2 and S3 of the Supporting Information). Below, we briefly discuss only those spectral regions that contribute more directly to the identification of the conformers or that are related

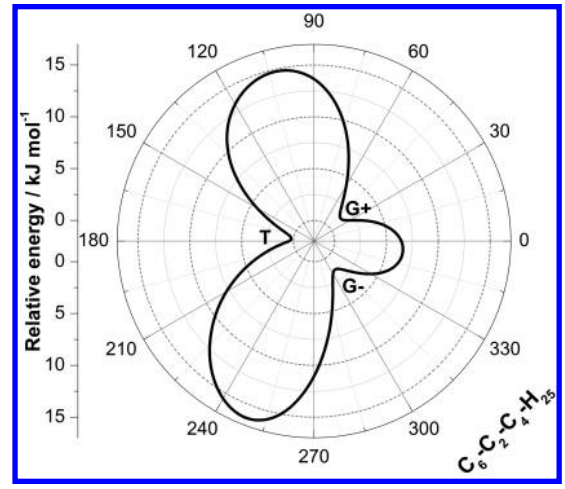

Figure 2. Calculated potential energy profile [DFT(B3LYP)/6311++G(d,p)] for interconversion between the conformers of α-terpinene. Minima are labeled by the conformer symbol (see Figure 1). The profile was obtained by performing a relaxed scan along the conformationally relevant torsional coordinate of the molecule ($C_6-C_2-C_4-H_{25}$ angle defining the internal rotation of the isopropyl group) by varying this coordinate in steps of 10° and optimizing all other coordinates.

to the molecular fragments that are expected to be directly involved in the photochemical reactions addressed later on in this article.

Monomeric α-terpinene has 72 vibrational modes. The IR spectrum is dominated by the strong absorptions due to 16 CH stretching vibrations. Thirteen out of 16 CH stretching modes have calculated IR intensities ranging from 20 to 80 km mol^{-1}; however, they occur in a very narrow frequency region and are not conformationally discriminative. Out of the remaining 56 vibrational modes in the fingerprint region, a maximum of four vibrations per conformer have calculated infrared intensities above 10 km mol^{-1}, and only one of these four vibrations (per conformer) is stronger than 14 km mol^{-1} (more precisely, it is 28 to 29 km mol^{-1}). Because of the low intrinsic intensities of its IR bands, α-terpinene is a difficult target for infrared spectroscopy studies, for example, requiring the usage of concentrated samples in matrix isolation studies. Indeed, usage of concentrated samples is a typical solution in infrared studies of molecules belonging to the family of CHD[43] or the corresponding open-ring analogue, 1,3,5-hexatriene.[44]

The fingerprint region of the IR spectra of monomeric α-terpinene is dominated by the band at ca. 825 cm^{-1} (in argon matrix; 823 cm^{-1} in xenon matrix) assigned to the CH out-of-plane wagging mode of the C═CH−CH═C fragment (calculated value: ∼830 cm^{-1} for all conformers). The medium intensity bands at 1663 and 1660 cm^{-1} (in argon and xenon matrices, respectively) are attributed to the antisymmetric C═C stretching vibration of the same fragment of the molecule (calcd: 1668−1670 cm^{-1} for all conformers). The band due to the symmetric C═C stretching vibration is predicted for all conformers at ca. 1617−1619 cm^{-1} with an intensity as low as 1 or 2 km mol^{-1}. This vibration was tentatively assigned to the weak bands observed at 1615 and 1613 cm^{-1} in argon and xenon matrices, respectively. In the diluted (argon) matrix, this band is practically buried below the absorption of the matrix water impurity. As it will be pointed out later on, the region of C═C stretching vibrations is important for the characterization of the photochemistry of the compound, although it is not suitable for discrimination of conformers.

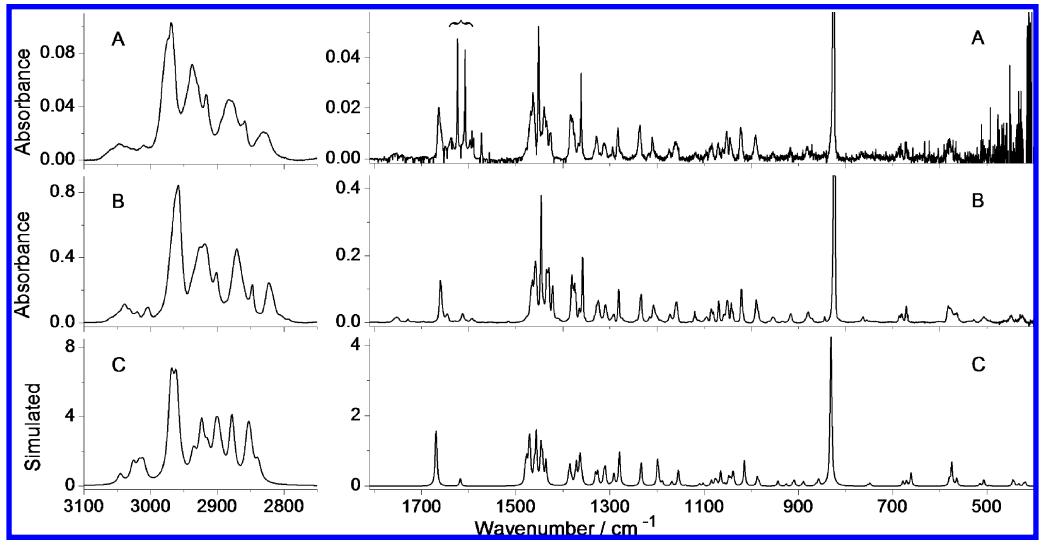

Figure 3. Experimental FTIR spectra of α-terpinene embedded in (A) argon (diluted matrix, 10 K) and (B) xenon (concentrated matrix, 20 K). (C) Simulated spectrum obtained as a sum of theoretical infrared spectra of the three conformers (G+, G−, T) with their intensities scaled proportionally to their estimated room-temperature gas-phase populations (G+/G−/T 22.8:22.2:55.0). The theoretical spectra in the CH stretching (3100−2750 cm^{-1}) and fingerprint (1800−400 cm^{-1}) regions were simulated by Lorentzian functions centered at the DFT(B3LYP)/6-311++G(d,p) calculated wavenumbers scaled by 0.960 and 0.978, respectively, and with fwhm equal to 10 and 4 cm^{-1}, respectively. The bracket in frame A designates absorptions due to the matrix-isolated monomeric water impurity. The band around 825 cm^{-1} is truncated in all spectra.

The bands that are the most distinct for the individual conformers of α-terpinene are observed in the 1340−1260 cm^{-1} and 690−650 cm^{-1} regions. According to the calculations, a vibration essentially characterized as a CH in-plane bending mode of the C═CH−CH═C moiety should be observed at 1280 (I = 11 km mol^{-1}), 1292 (I = 4.2 km mol^{-1}) and 1292 (I = 4.7 km mol^{-1}) cm^{-1}, for T, G+ and G− conformers, respectively. The experimental bands originating from this mode are indeed observed at 1283/1281 cm^{-1} (strong; Ar/Xe) for the Trans conformer and at 1295/1292 cm^{-1} (weak; Ar/Xe) for the Gauche conformers. (See Table S3 of the Supporting Information.) Additionally, the calculations predicted pairs of intense bands at 1331/1311 cm^{-1} and 1326/1312 cm^{-1}, which are mainly due to the CH_2 wagging mode of the C−CH_2−C moities of the G+ and G− conformers, respectively, whereas the corresponding bands of the Trans form are predicted at 1329/1310 cm^{-1} with very low intensities. Therefore, the experimental IR bands at 1328/1325 (strong; Ar/Xe) and 1312/1310 cm^{-1} (strong, Ar/Xe) were assigned to the CH_2 wagging mode and taken as conformer discriminative bands mainly due to the two Gauche forms.

According to the calculations, in the much extended 750−600 cm^{-1} region, only one vibration per conformer is expected. They are predicted by the DFT calculations to appear well separated at 679, 671, and 661 cm^{-1} for G+, G−, and T, respectively. This fact makes this spectral region a suitable probe for conformers of α-terpinene. It must be noted, however, that the calculated infrared intensities of these bands range from 3.7 to 4.2 kJ mol^{-1}, which require rather concentrated samples for their reliable experimental observation. The experimental bands are observed at 686, 682, and 671 cm^{-1} in the spectra of the concentrated matrices. In the diluted matrices, these bands have intensities of the level of the instrumental noise. Nevertheless, this is indeed the sole spectral region where well-separated bands due to only T, G+, or G− could be unequivocally observed (in the concentrated matrices); therefore, it is of particular importance for searching for the presence of the individual conformers in the trapped conformational mixture.

The calculations also predicted some other modes to appear at sufficiently distant wavenumbers in the different conformers, so as to be potential conformational markers, but these were found to be nonapplicable in practical terms because they either occur in crowded spectral regions or have too low intensity.

Conformational Preferences of α-Terpinene in the Condensed Phase. The comparison of the FTIR-ATR spectrum of liquid α-terpinene with the IR spectra obtained for the compound isolated in the inert gas matrices shows relevant differences, in particular, regarding band intensities. (See Figure 4.) This comparison suggests that the conformational equilibrium found for the room-temperature gas phase is considerably different from that present in the liquid at the same temperature.

To characterize conformationally the liquid phase, spectroscopic results obtained for α-terpinene in xenon and argon matrices under different concentrations were of key importance. For each matrix gas, two samples were prepared, one diluted and the other one considerably more concentrated. Both xenon and argon matrices were then annealed.

In principle, one could expect that annealing of a diluted matrix may reveal some relaxation of both higher energy Gauche forms into the most stable Trans conformer. However, the performed annealing of argon matrix up to 30 K did not lead to any spectral changes that could be ascribed to any conformational isomerization. The contributions of these two types of conformers to the spectra then remain unchanged, indicating that their relative populations were not modified.

A different behavior was observed during the experiments carried out for α-terpinene isolated in xenon matrices. Annealing up to 35 K did not lead to any spectral changes, indicating that up to this temperature, the relative populations of conformers were not modified, which is in agreement with the experiments carried out for the argon matrix. However, significant redistribution of band intensities was found to take place between 40 and 60 K. Figure 5 shows the observed changes in the conformer-sensitive spectral regions. As can be noticed, in the 1260−1340 cm^{-1} range, the intensity of the bands ascribable to the Gauche conformers (1292, 1325/1328, and, to less extent, 1310 cm^{-1}) increases, whereas that of the band due to the Trans conformer (1281 cm^{-1}) significantly decreases with the increase of temperature. Note that the expected contribution of the T conformer to the band at ca. 1310 cm^{-1} is relatively larger than

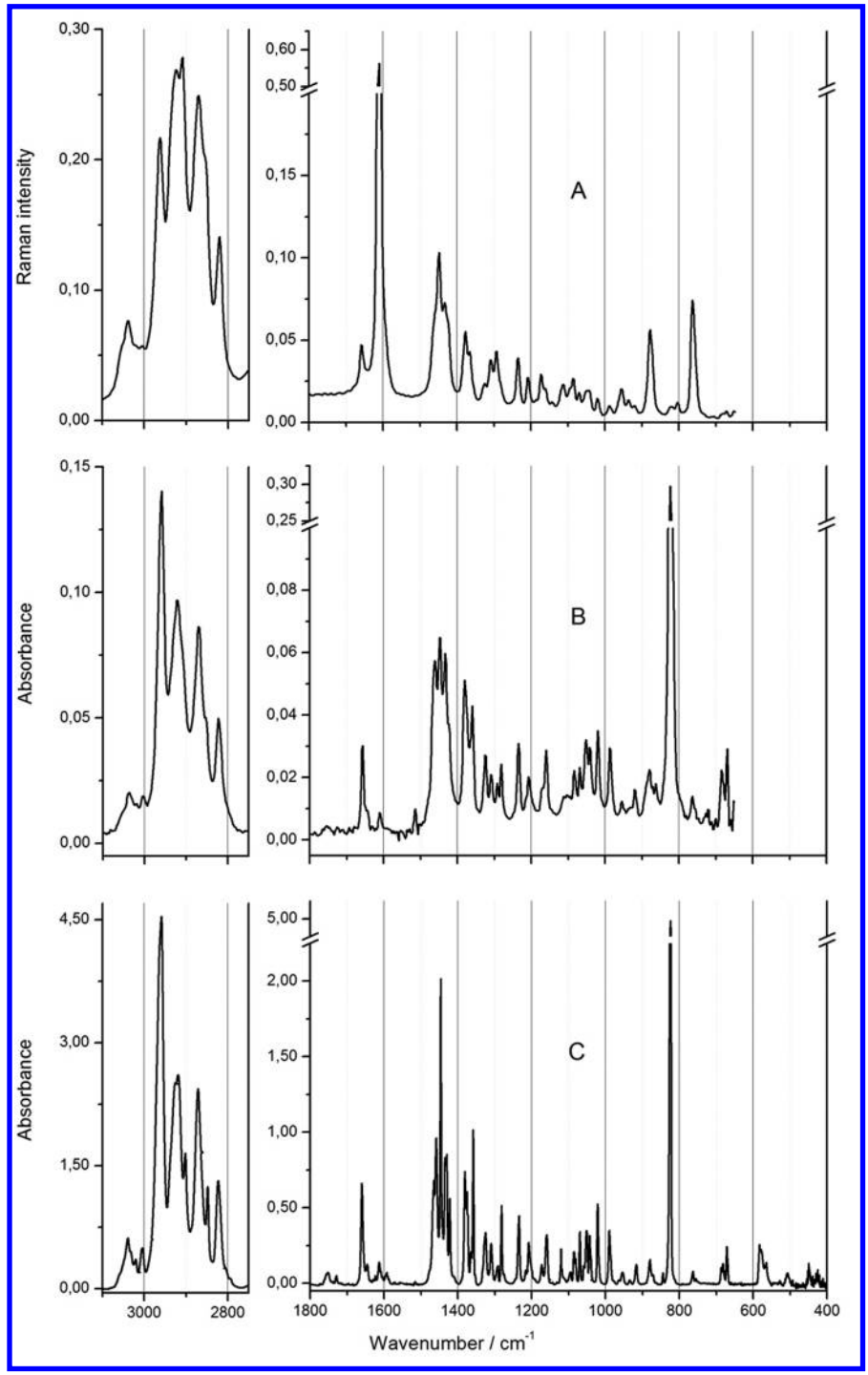

Figure 4. Experimental (A) FT-Raman and (B) FTIR-ATR spectra of the liquid α-terpinene at room temperature and (C) FTIR spectra of α-terpinene in a concentrated xenon matrix in the 3100−2700 and 1800−400 cm^{-1} regions.

that for the bands at 1325/1328 cm^{-1} (Table S3 of the Supporting Information), justifying the much smaller intensity changes for the first band. Values of the integral intensities of the bands, which were more affected by the annealing (using as internal reference the 1159 cm^{-1} band, which does not change intensity with temperature), showed that the population of conformer T decreases from 55 to ca. 26% of the total, whereas, those of G+ and G− increase by ca. 13% each when the temperature of the matrix was increased from 40 to 60 K; that is, the G+/G−/T population ratio changed from 0.228:0.222:0.550 to 0.358:0.352:0.290. These results indicate that approximately half of the deposited Trans molecules convert to the Gauche forms upon annealing up to 60 K.

The point to stress is that the conformational redistribution shifts in the opposite direction relatively to what could be expected. In the freshly deposited matrices, the room-temperature gas-phase equilibrium was trapped as a metastable state at the matrix temperature (20 or 30 K). Then, annealing of a diluted matrix should promote relaxation of the conformational distribution toward the low-temperature equilibrium.[45] On the basis of our theoretical calculations for monomers in vacuo, this corresponds to the Gauche → Trans conversion and not to the experimentally observed opposite process.

For the concentrated sample, this observation can be interpreted as follows: an increase in the matrix temperature allows for the occurrence of partial molecular diffusion. This leads to

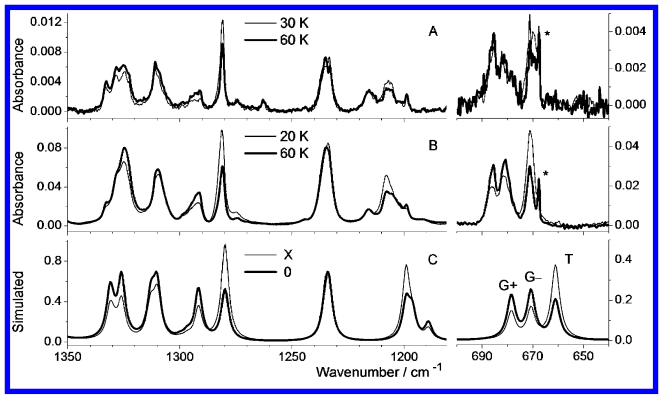

Figure 5. Experimental FTIR spectra of α-terpinene in (A) diluted and (B) concentrated xenon matrix recorded immediately after deposition (thin line) and after annealing of the samples to 60 K (bold line). Asterisks designate absorption due to the atmospheric CO_2. (C) Spectra of conformational mixtures were simulated with Lorentzian functions (fwhm = 4 cm^{-1}) centered at the calculated DFT(B3LYP)/6-311++G(d,p) frequencies and scaled by 0.978. Theoretical intensities in spectrum "X" (thin line) were scaled to the predicted populations of conformers T, G+, and G− expected for their equilibrium mixture at room temperature: (55.0% T) + (22.8% G+) + (22.2% G−). Theoretical intensities in spectrum "0" (bold line) were scaled assuming that about half of the initial amount of T from (26%) was consumed and converted equally to G+ and G− (13% each). The corresponding scaling factors were: (29.0% T) + (35.8% G+) + (35.2% G−). Signatures of the individual conformers are indicated in the 700−650 cm^{-1} region. Please note the abscissa break.

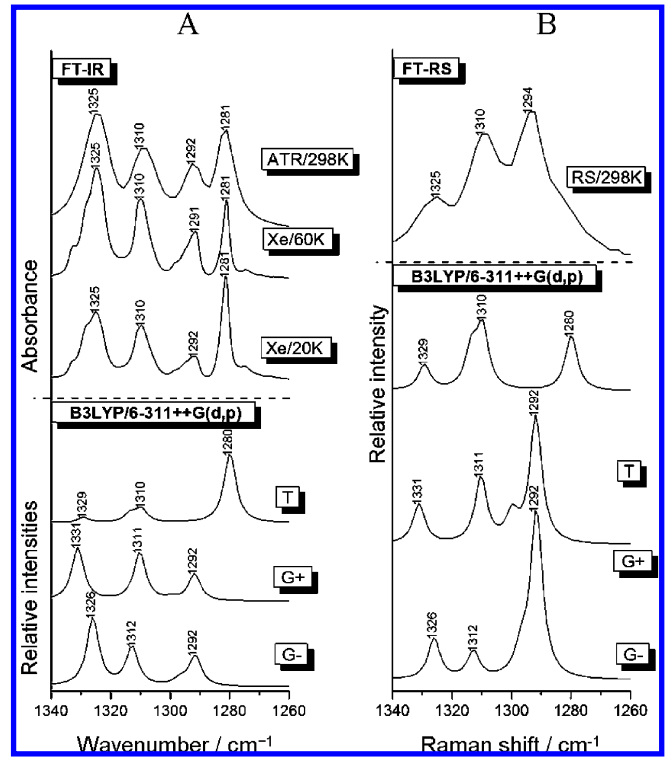

Figure 6. (A) Comparison of the IR spectra of the concentrated sample of α-terpinene isolated in the xenon matrix during annealing at 20 and 60 K with the FTIR-ATR spectrum of the liquid α-terpinene (top frame) and the calculated IR spectra for all conformers (bottom frame). (B) Comparison between the FT-Raman spectrum of the liquid α-terpinene (top frame) and calculated Raman spectra for all conformers of α-terpinene (bottom frame). The theoretical spectra were calculated at the DFT(B3LYP)/6-311++G(d,p) level, and wavenumbers were scaled by 0.978.

the appearance of relevant intermolecular interactions between the closely located molecules of the solute, which seem to favor the Gauche conformers. The Gauche forms then become considerably stabilized in relation to the Trans conformer under these experimental conditions. Such stabilization provides the driving force for the conformational isomerization of Trans into Gauche forms.

In accordance with this interpretation, the FTIR-ATR spectrum of neat α-terpinene at room temperature shows a profile in the 1260−1340 cm^{-1} conformer-sensitive region that follows the same trend as that exhibited by the spectra of the annealed matrices (Figure 6A), clearly revealing an enrichment of the population of the Gauche conformers in relation to that trapped in the nonannealed matrix. Furthermore, the comparison between the experimental FT-Raman spectrum of α-terpinene at room temperature (the full spectrum is presented in Figure 4) and the theoretical Raman spectra of the α-terpinene conformers in the 1260−1340 cm^{-1} spectral region (Figure 6B) also shows that in the neat liquid the Gauche conformers of α-terpinene are clearly dominant. We estimated the population of the conformers in the liquid at room temperature by using the conformationally sensitive spectral region of the FTIR-ATR and FT-Raman spectra. Because of difficulties in the separation of the G+/G− bands, only the (G+/G−)/T ratio could be determined, being 0.70:0.30 (equal in practical terms to that found in the annealed concentrated xenon matrix, 0.71:0.29, and substantially different from that existing in the gas phase, 0.45:0.55).

For the diluted samples, the solute−solute interactions can be neglected. However, to explain the unexpected direction of the conformational changes also for diluted matrices, we resorted to the PCM calculations in the argon solvent. These calculations show stabilization of both Gauche forms with respect to T, in particular, G−. The values of the total free energy of Gauche forms (G−/G+, respectively), compared with Trans, decrease from 1.41/1.34 (for vacuum) to 1.01/1.33 kJ mol^{-1} (for the argon solvent). Moreover, the trend in the series of argon−krypton−CCl_4 suggests a further stabilization of the Gauche forms in more polarizable media, which agrees with the experimental observations.

Photochemical Behavior of Matrix-Isolated α-Terpinene. Matrix-isolated α-terpinene was subjected to a series of UV irradiations using different cutoff filters. For irradiations with wavelengths longer than 283 nm, no changes were observed in the spectrum. This is consistent with the UV-absorption spectrum of the parent molecule (CHD)[20] as well as that of α-terpinene,[29] which do not absorb above 280 nm. The irradiation at $\lambda > 235$ nm (where both CHD and α-terpinene exhibit their main absorptions) led to the emergence of new bands, whose intensities increase significantly in the initial stages of irradiation. These results show that α-terpinene is photolabile in the range of germicidal UV−C light only.

In an attempt to identify the photoproducts of the (UV−C)-irradiated α-terpinene, the spectral region of the C═C stretching modes (1550−1700 cm^{-1}) was examined. The comparison between the FTIR spectra of α-terpinene and of those of its photoproduct(s) in this range (Figure 7) shows significant changes, indicating rearrangement of the π system of the molecule after reaction. In particular, the sole strong ν(C═C) band observed in the spectrum of α-terpinene (1660 cm^{-1}) is replaced in the spectrum of the irradiated matrix by two strong bands at 1626 and 1595 cm^{-1}. The observation of the two main bands in this spectral range points either to the existence of more than one photoproduct or to a photoproduct structure that contains an additional double bond compared with the irradiation substrate. Also, the presence of three C═C double bonds in the photoproduced species is consistent with the occurrence of the

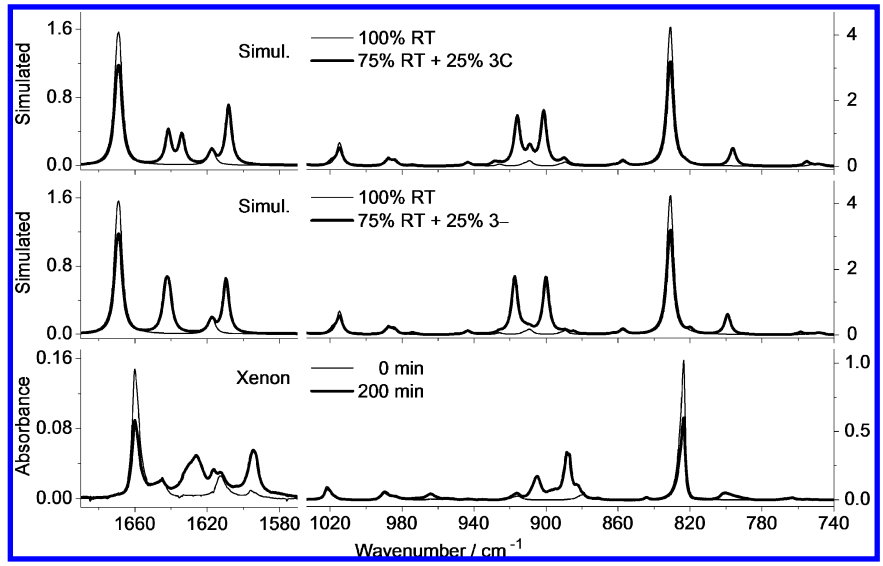

Figure 7. Bottom frame: Experimental FTIR spectra of α-terpinene in concentrated xenon matrix before (thin line) and after UV ($\lambda > 235$ nm) irradiation (bold line). Middle and top frames: Simulated infrared spectrum of the equilibrium mixture of the conformers at room temperature (100% RT, thin line) compared with simulated spectra of the selected open-ring isomers. In the simulations of the irradiation (bold lines), the intensity of substrate absorption (RT) was reduced to 75%, and the resulting scaled spectrum was coadded with the spectrum of the chosen open-ring product (3−, 3C), which was reduced to 25%. The abbreviated names 3− and 3C stand for tZg+/SK− and tZg+/C, respectively. (See also Table 2 and Figure 8.) Please note the abscissa break. In this spectral range, the spectrum of conformer 3+ (tZg+/SK+) is practically coincident with that of form 3C.

TABLE 2: Structural and Energetic Parameters of α-Terpinene Conformers and of the Corresponding Open-Ring Isomers Calculated at the DFT(B3LYP)/6-311++G(d,p) Level of Theory[a]

complete conformer name	short name	dihedral angles A	B	C	D	|μ|	relative energy $\Delta E°$	$\Delta E°_{ZPVE}$	$\Delta G°$
trans	**T**				173.4	0.54	0.00	0.00	0.00
gauche−	**G−**				−53.8	0.65	1.41	1.75	2.25
gauche+	**G+**				40.7	0.63	1.34	1.76	2.18
g+Zg+/C	**1C**	52.0	4.2	46.8	−4.2	0.18	100.5	91.3	83.3
g+Zg+/SK+	**1+**	49.5	4.4	47.2	128.9	0.25	100.4	91.7	85.3
g+Zg+/SK−	**1−**	51.2	3.2	48.4	−143.1	0.22	103.3	94.4	86.0
g+Zg−/C	**2C**	47.1	−2.7	−70.7	1.1	0.68	103.8	95.1	86.7
g+Zg−/SK−	**2−**	45.3	−2.9	−67.6	−131.1	0.73	104.3	95.9	87.7
tZg+/C	**3C**	−170.9	8.2	53.8	−4.9	0.61	94.3	86.7	80.8
tZg+/SK−	**3+**	−172.5	6.9	60.6	−136.8	0.69	97.0	89.9	82.3
tZg+/SK+	**3−**	−171.3	8.4	54.7	127.7	0.62	94.2	87.2	82.1
g+Zt/SK+	**4+**	42.8	6.1	−140.7	144.5	0.71	99.1	90.9	83.5
tEg+/C	**5C**	−179.9	−178.7	33.1	−5.2	0.65	69.0	60.9	54.9
tEg+/SK+	**5+**	−179.5	−178.5	34.2	131.1	0.71	69.2	61.9	57.0
tEg+/SK−	**5−**	−179.7	−179.8	30.5	−141.9	0.73	71.3	63.9	58.6
g+Eg+/C	**6C**	34.3	−177.7	34.9	−4.0	0.46	80.9	71.9	65.3
g+Eg+/SK+	**6+**	34.3	−177.5	35.4	131.0	0.47	81.3	72.9	66.9
g+Eg+/SK−	**6−**	34.7	−179.2	33.0	−141.8	0.51	83.5	74.7	67.9
g+Et/C	**7C**	33.3	−178.9	−179.9	−0.5	0.65	81.7	73.9	68.2
g+Et/SK+	**7+**	33.8	−179.8	−175.7	141.2	0.69	74.8	66.9	61.4
g+Et/SK−	**7−**	33.3	−178.3	177.7	−143.6	0.69	75.1	67.4	61.7
tEt/C	**8C**	180.0	180.0	180.0	0.0	0.15	69.1	62.1	57.7
tEt/SK−	**8−**	−179.9	−179.3	177.2	−142.1	0.06	62.2	55.8	51.9

[a] DFT(B3LYP)/6-311++G(d,p) calculated energies of the closed-ring Trans conformer of α-terpinene were chosen as the zero level. The relative calculated energies of the remaining forms are given in kilojoules per mole. The corresponding absolute energies of T conformer are given in the caption of Table 1. Dipole moments (|μ|/debye). Dihedral angles A, B, C, D (degrees) stand for (methyl side) $H_2C{=}C{-}C{=}C$, $C{-}C{=}C{-}C$, $C{=}C{-}C{=}CH_2$ (isopropyl side), and $C{=}C{-}C{-}H$ (isopropyl), respectively. For the closed-ring molecule, the values of dihedral angle D (defining orientation of the isopropyl group) refer to the $H_2C{-}C{-}C{-}H$ angle. In the abbreviated names, the backbone structure is designated by an Arabic numeral followed by + (skew+), − (skew−) or C (cis), defining the orientation of isopropyl group.

ring-opening process analogous to those observed for CHD[22,23,25−32,43] and α-terpinene in the gas phase.[29]

The analysis of the 750−1050 cm^{-1} spectral range (Figures 7 and 8) gives further support to this conclusion. Indeed, the strong IR band of α-terpinene at ca. 820 cm^{-1}, ascribed to the CH out-of-plane wagging mode of the ring $C{=}C(9)H{-}C(10)H{=}C$ fragment, decreases upon irradiation, whereas new bands at ca. 800 cm^{-1} and in the 888−910 cm^{-1} range emerge. The new bands are ascribable to the CH out-of-plane wagging mode of the rearranged $C{-}C(9)H{=}C(10)H{-}C$ fragment, and the wagging vibration of the $=CH_2$ group of the open-ring isomeric species, respectively, which are absent in α-terpinene (see

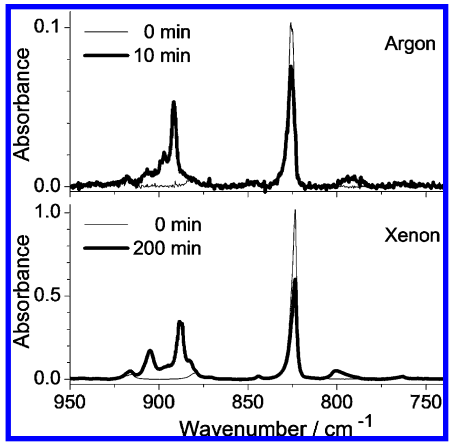

Figure 8. Changes in the experimental FTIR spectra caused by UV irradiation ($\lambda > 235$ nm) of α-terpinene isolated in the concentrated xenon matrix (at 50 K, bottom frame) and the diluted argon matrix (at 10 K, top frame). The similarity of changes suggests that the photochemistry does not depend very much on the nature of the matrix host atoms or on the concentration.

Scheme 1). Similarly, very strong infrared bands were observed at 900 and 890 cm^{-1} for a related compound, 2,5-dimethyl-1,3,5-hexatriene, isolated in an argon matrix.[44]

To characterize the resulting photoproduct(s) structurally in more detail, we carried out an extensive series of theoretical calculations on the various possible open-ring isomers of α-terpinene. This provided relevant structural and energetic data as well as vibrational information crucial for the analysis of the spectra of the irradiated matrices and detailed identification of the photoproduced species.

The nomenclature to name the open-ring structures derived from α-terpinene uses as a starting point that of the parent molecular system, 1,3,5-hexatriene (HT), which is the open-ring isomer of CHD. The ring-opening of cyclohexadiene is nowadays one of the experimentally and theoretically best documented photochemical reactions.[20−23,25−32,46−54]

The structures of HT are commonly named cZc, cZt, tZt, cEc, tEt, and so on. In this symbolic code, the central capital letter, Z or E, defines the configuration around the central C═C bond, whereas the terminal letters, c or t, define the orientation around the adjacent CC single bonds. However, this nomenclature is oversimplified because most of the Z isomers of HT are nonplanar, and the c names actually correspond to the gauche (g) orientations, whereas t actually corresponds to Trans. In such an intrinsically symmetric system as HT, usage of the c symbolic code (in place of g) does not induce any ambiguity. In the present study, the HT-like open-ring backbone of α-terpinene's photoproduct bears an isopropyl group at position two, which renders nonequivalent g− and g+ positions.

The nomenclature here adopted was then slightly modified. The capital letter, Z or E, defines the configuration around the central C═C bond, in the same way as in HT. For each of the Z or E structures, nine reference structures with Trans (t) or gauche (g+; g−) arrangements of the two C═C−C═C moieties can be devised. (See Figure 9 and Figure S1 in the Supporting Information, which is an extended version of Figure 9.) Furthermore, each structure defined by the configuration around the central C═C, C(2)−C(6), and C(7)−C(8) bonds (Figure 1) may have three different arrangements of the isopropyl group H−C(4)−C(2)−C(6): Cis (0°; C), Skew+ (+120°; SK+), and Skew− (−120°; SK−). These letter codes are ordered starting from the methyl end of the open-ring product toward its isopropyl end.

It is important to stress here that the anchor carbon atom defining the orientation of the isopropyl group in the closed ring molecule (T, G+, and G−), is kept the same for the definition of the isopropyl orientation in the open-ring structures. Because of the fact that formally single and double bonds interchange in the ring-opening reaction, the isopropyl group makes an additional rotation (ca. 60°) in the process. Then, assuming the minimal rotation from the T, G+, and G− positions, the SK−, C, and SK+ orientations arise if the rotation is counter-clockwise (CCW), or SK+, SK−, and C arise if the rotation is clockwise (CW). The possibility of the relaxation of the open ring structure in two directions is a premise for the conformational branching during the photochemistry.

On the whole, the number of nonequivalent by symmetry reference structures considered is 28. With a single exception (the fully distended t*Et*/C form; see Figure 9), none of these reference structures were found to be minima on the potential energy surface of the molecule. The minimum energy structures, however, are designated here using the notation of the closest resembling reference structure for simplicity. Twenty different minima could be found on the molecule's PES, corresponding to 11 E-type structures and 9 Z-type structures. The minimum energy structures and their defining dihedral angles, dipole moments, and relative energies are given in Table 2. The E-type conformers were predicted by the calculations to be considerably more stable than the Z-type structures, with the more extended tEg+/C and tEt/SK− conformers being the most stable species.

Figure 10 shows the theoretical stick spectra of α-terpinene (bottom frame) and its possible open-ring isomers calculated at the DFT(B3LYP)/6-311++G(d,p) level of theory. Note that the Figure does not intend to provide information on a particular isomer but rather concentrates on isomer types. The isomers considered in this analysis were chosen by the analogy to the photochemistry of α-pyrone.[24] Therefore, besides Z and E open-ring isomers, the Figure also shows the calculated spectrum for the Dewar isomer of α-terpinene (top frame).

The out-of-plane vibrations of the two central CH groups (shown explicitly in the structural schemes presented on the right side of Figure 10) have the strongest infrared intensities in this spectral region and can be used as spectral markers in discriminating different isomers. Note that the ordinate scales in the Figure are equal in all frames, showing that infrared intensities of the photoproducts are slightly higher than those in the starting compound. The main conclusions extracted from Figure 10 are the following:

(i) The Dewar isomer of α-terpinene (which might exist in three different conformational states differing by the orientation of the isopropyl substituent) is predicted to give rise to an intense band (due to the out-of-plane bending vibration of the CH groups attached to the central C═C bond) at ca. 750 cm^{-1}. In the experimental spectra, no such band could be found (Figure 7), doubtlessly confirming that the Dewar isomer is not formed upon irradiation of matrix-isolated α-terpinene and then that the ring-contraction pathway is not operative in this molecule, contrarily to what has been previously found for α-pyrones[24] and other analogous molecules, such as methyl coumalate.[55] Indeed, for α-terpinene, the Dewar isomer is sterically crowded and energetically unfavorable because of the presence of the two bulky substituents, methyl and isopropyl groups, which should be in close proximity.

(ii) The open-ring *E*-type forms are predicted to give rise to intense bands around 900 and 1000 cm^{-1}. The Z-type forms have a signature characterized by the presence of intense bands at ca. 800 and 900 cm^{-1}. The absence of new bands around

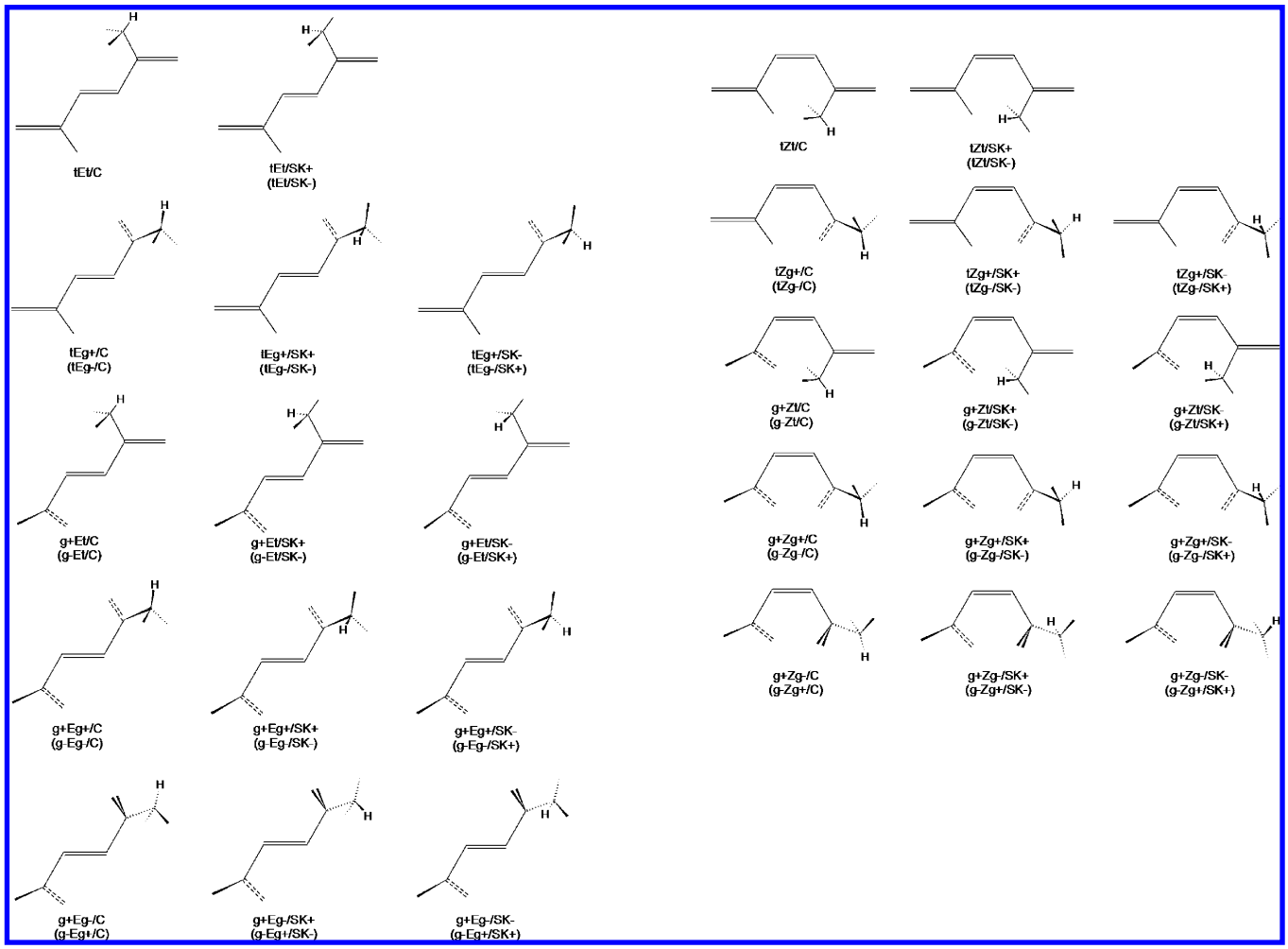

Figure 9. Reference structures and notation adopted to name the open-ring isomers of α-terpinene. The capital letter, Z or E, defines the configuration around the central C═C bond. For each of the Z or E structures, nine reference structures with Trans (t) or Gauche (g+; g−) arrangements of the two C═C−C═C moieties exist, which in turn may have three different arrangements of the isopropyl group [Cis (H−C(4)−C(2)−C(6), 0°; C], Skew+ (+120°; SK+) and Skew− (−120°; SK−). These letter codes are ordered starting from the methyl end toward the isopropyl end of the molecule. The names of symmetry-equivalent mirror images are given in parentheses in this Figure and shown explicitly in the extended version of the Figure provided as Supporting Information (Figure S1).

1000 cm^{-1} (Figure 7) is an indication that the formation of the E isomer is suppressed in photochemistry of matrix-isolated α-terpinene. The expected spectral profile for Z-type forms shown in Figure 10 matches very well the experimental profile (Figure 7). It can then be concluded that the clearly dominant observed photochemistry is the ring-opening reaction with predominant formation of the Z isomer.

(iii) The identification of the particular conformer(s) generated in the photoreaction is difficult because the predicted spectra of the different conformers are quite similar. However, a prevalence of the open-ring isomers with the tZg backbone seems to be very likely based on the close match between the experimentally observed spectrum and the simulation. (See Figure 7; the full spectra assignment is presented in Tables S4 and S5 of the Supporting Information.) These are among the conformers that could be expected to result from the open-ring reaction with the smallest structural rearrangement. This observation for α-terpinene is consistent with the principle of least motion,[56] which has been formulated in the context of the ring-opening reaction in related compounds. This last fact is certainly an important issue because an extensive structural rearrangement would imply a simultaneous major rearrangement of the matrix, which is an energetically demanding process.

Some additional conclusions can be extracted from the obtained photochemical results. First, the analysis of the 700−650 cm^{-1} conformer-sensitive spectral region indicates that all individual α-terpinene conformers (T, G+, G−) are consumed in the photoreaction. Second, it was found that the photochemical reactions in argon and xenon matrices are qualitatively similar (see Figure 8). The absence of the heavy atom effect due to xenon is in agreement with the expected mechanism of the photoprocess, a typical concerted $\sigma^2 + \pi^4$ electrocyclic ring-opening conrotatory reaction taking place in S_1 (according to the Woodward−Hoffmann orbital symmetry rules[57]).

The sole production of Z conformers of the photoproduct of α-terpinene is in line with the photochemistry of matrix-isolated CHD, which was found to undergo rapid photolysis to the Z open-ring structures.[43] An important paradigm in the triene photochemistry has been the nonequilibration of excited rotamers (NEER) principle, which notes that equilibration of the excited rotamers during the singlet-excited state lifetime does not occur, implying unique photochemistry and photophysics for each rotamer.[44] If the photoisomerization of each conformer was highly stereoselective giving the product anticipated in a model emphasizing ground-state geometry as a stereochemical determinant and accounting for the principle of least motion,[56] then two different conformers with a given backbone type and different isopropyl group orientation should be produced from each conformer of α-terpinene (for CCW and CW rotation of

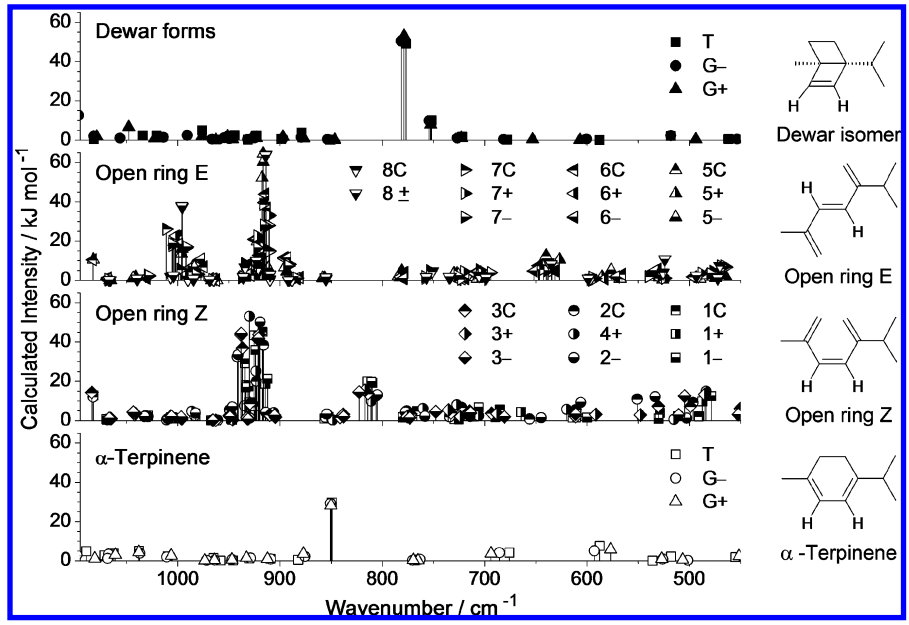

Figure 10. Theoretical stick spectra of α-terpinene (bottom frame) and its possible isomers calculated at the DFT(B3LYP)/6-311++G(d,p) level of theory. The out-of-plane vibrations of the two central CH groups (shown explicitly on the right side of the Figure) have the strongest infrared intensities in this spectral region and can be used as spectral markers discriminating different isomers. The calculated frequencies and intensities are not scaled. Note that ordinate scales are equal in all frames. The Arabic numerals in the two middle frames stand for the abbreviated backbone type, and the symbols +, −, and C stand for the orientation of the isopropyl group, SK+, SK−, and Cis, respectively. The full conformational names are shown in Table 2 and Figure 9.

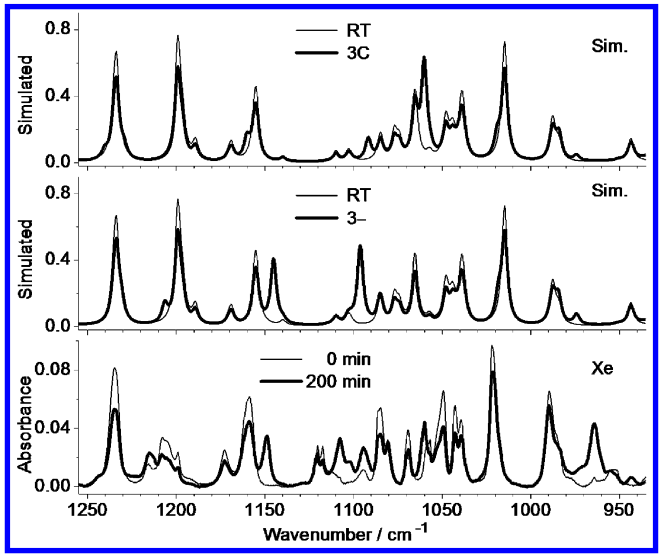

Figure 11. Bottom frame: Experimental FTIR spectra of α-terpinene in concentrated xenon matrix before (thin line) and after UV ($\lambda > 235$ nm) irradiation (bold line). Middle and top frames show the simulated infrared spectrum of the equilibrium mixture of the conformers at room temperature (RT, thin line) compared with simulated spectra of the selected open-ring isomers, 3− and 3C. The abbreviated names 3− and 3C stand for tZg+/SK− and tZg+/C, respectively. (See also Table 2 and Figure 9.) In this spectral range, the spectrum of conformer 3+ (tZg+/SK+) is practically coincident with that of form 3−.

the isopropyl fragment). On the whole, all six tZg-type conformers of the open-ring photoproduct (Figure 9) must then be produced. This is in agreement with the spectroscopic data shown in Figures 7 and 11 showing that structures 3C, 3+, and 3− exhibit infrared spectra that are congruous with the experimental spectrum of the photoproduct.

Conclusions

In the current study, the conformational space and photochemistry of α-terpinene were explored. The conformers and barriers for conformational isomerization were calculated at the DFT(B3LYP)/6-311++G(d,p) level of theory. According to these calculations, in the gas phase, the Trans conformer was predicted to be more stable than the Gauche forms, with the G+/G−/T population ratio being ca. 1:1:2.5, at room temperature. The theoretical predictions were fully confirmed by analysis of the infrared spectra of the compound isolated in argon and xenon cryogenic matrices, where the gas-phase equilibrium could be efficiently trapped at temperatures below 30 K because of the relatively high energy barriers separating conformers that prevent conformational changes during the matrix deposition.

Annealing of the samples to temperatures of ∼50 K (possible only in the case of xenon matrices) introduced changes in the spectra that can be attributed to conformational isomerization. Contrary to what could be expected from the theoretically calculated relative energies of the conformers, the conformational changes occurred from the Trans to the Gauche forms. These observations point to the stabilization of the Gauche forms in the matrices. Stabilization of the Gauche conformers was also evidenced for the liquid compound by analysis of the conformer-sensitive spectral regions using both infrared and Raman techniques. According to these observations, theoretical calculations using the PCM approach showed stabilization of both Gauche forms with respect to Trans in solutions in comparison with vacuum.

Exposure of the matrix-isolated α-terpinene to UV−C light was found to induce a concerted $\sigma^2 + \pi^4$ electrocyclic ring-opening reaction, taking place in S_1 and leading to the formation of an α-terpinene open-ring isomer in the Z configuration. It is suggested that the dominant conformers of the photoproduct resulting from photolysis have the tZg backbone, whose formation requires only relatively small structural rearrangements of both the reagent and matrix. As for α-terpinene parent molecule CHD, but contrarily to what has been observed for similar molecules like α-pyrones and substituted analogues, the putative photochemical process leading to ring contraction and

formation of the Dewar isomer was found to be not operative for α-terpinene under the experimental conditions used.

Acknowledgment. This work was supported by FCT (project PTDC/QUI/71203/2006) and by The Polish State Committee for Scientific Research (KBN), 2009/2011 (grant no. N N204 341437). We would also like to thank Prof. Małgorzata Barańska (The Jagiellonian University) for recording the FTIR-ATR spectrum of α-terpinene.

Supporting Information Available: Reference structures and notation adopted to name the open-ring isomers of α-terpinene, structural parameters of Trans, Gauche+, and Gauche− conformers of α-terpinene calculated at the DFT(B3LYP)/6-311++G(d,p) level of theory, definition of internal coordinates used in the normal coordinate analysis of α-terpinene and the open-ring isomers of α-terpinene, experimental wavenumbers and intensities of the infrared spectra of α-terpinene isolated in argon and xenon matrices compared with the calculated infrared spectra with potential energy distribution for the three conformers of the molecule, and experimental wavenumbers and intensities of the infrared spectra of the open-ring isomers of α-terpinene photogenerated in argon and xenon matrices by UV irradiation compared with the infrared spectra calculated at the DFT(B3LYP)/6-311++G(d,p) level of theory with potential energy distribution for the three conformers of the open-ring photoproduct with the tZg+ backbone. This material is available free of charge via the Internet at http://pubs.acs.org.

References and Notes

(1) Schultz, H.; Barańska, M. *Vib. Spectrosc.* **2007**, *43*, 13–25.
(2) Matura, M.; Skold, M.; Borje, A.; Andersen, K. E.; Bruze, M.; Frosch, P.; Goossens, A.; Johansen, J. D.; Svedman, C.; White, I. R.; Karlberg, A. T. *Am. J. Contact Dermatitis* **2005**, *52*, 320–328.
(3) Farag, R. S.; Daw, Z. Y.; Hewedi, F. M.; El-Baroty, G. S. A. *J. Food Prot.* **1989**, *52*, 665–667.
(4) Breitmaier, E. *Terpenes: Flavors, Fragrances, Pharmaca, Pheromones*; Wiley-VCH: Weinheim, Germany, 2006.
(5) Sefidkon, F.; Jamzad, Z.; Mirza, M. *J. Food Chem.* **2004**, *88*, 325–328.
(6) Cheng, S.; Liu, J.; Hsui, Y.; Chang, S. *Bioresour. Technol.* **2006**, *97*, 306–312.
(7) Nhu-Trang, T.-T.; Casabianca, H.; Grenier-Loustalot, M.-F. *J. Chromatogr., A* **2006**, *1132*, 219–227.
(8) Al-Burtamani, S. K. S.; Fatope, M. O.; Marwah, R. G.; Onifade, A. K.; Al-Saidi, A. S. H. *J. Ethnopharmacol.* **2005**, *96*, 107–112.
(9) Mahmoud, A. A.; Ahmed, A. A. *Phytochemicals* **2006**, *67*, 2103–2109.
(10) Schulz, H.; Ozkan, G.; Barańska, M.; Kruger, H.; Ozcan, M. *Vib. Spectrosc.* **2005**, *39*, 249–259.
(11) Schulz, H.; Quilitzsch, R.; Kruger, H. *J. Mol. Struct.* **2003**, *661*−*662*, 299–306.
(12) Harkenthal, M.; Reichling, J.; Geiss, H. K.; Saller, R. *Pharm. Ztg.* **1998**, *143*, 26–30.
(13) Gallivan, J. B.; Brinen, J. S. *Chem. Phys. Lett.* **1971**, *10*, 455–459.
(14) Land, E. J.; Truscott, T. G. *Photochem. Photobiol.* **1979**, *29*, 861–866.
(15) Iwanami, Y.; Tateba, H.; Kodama, N.; Kishino, K. *J. Agric. Food Chem.* **1997**, *45*, 463–466.
(16) Avcibaşi, N.; Içli, S.; Gilbert, A. *Turk. J. Chem.* **2003**, *27*, 1–7.
(17) Hausen, B. M.; Reichling, J.; Harkenthal, M. *Am. J. Contact Dermatitis* **1999**, *10*, 68–77.
(18) Karapire, C.; Kolancilar, H.; Oyman, U.; Içli, S. *J. Photochem. Photobiol., A* **2002**, *153*, 173–184.
(19) Celani, P.; Bernardi, F.; Robb, M. A.; Olivucci, M. *J. Phys. Chem.* **1996**, *100*, 19364–19366.
(20) Harris, D. A.; Orozco, M. B.; Sension, R. J. *J. Phys. Chem. A* **2006**, *110*, 9325–9333.
(21) Dou, Y.; Yuan, S.; Lo, G. V. *Appl. Surf. Sci.* **2007**, *253*, 6404–6408.
(22) Kuthirummal, N.; Rudakov, F. M.; Evans, C. L.; Weber, P. M. *J. Chem. Phys.* **2006**, *125*, 133307.
(23) Carroll, E. C.; Pearson, B. J.; Florean, A. C.; Bucksbaum, P. H.; Sension, R. J. *J. Chem. Phys.* **2006**, *124*, 114506.
(24) Breda, S.; Reva, I. D.; Lapinski, L.; Fausto, R. *Phys. Chem. Chem. Phys.* **2004**, *6*, 929–937.
(25) Fuβ, W.; Schikarski, T.; Schmid, W. E.; Trushin, S.; Kompa, K. L. *Chem. Phys. Lett.* **1996**, *262*, 675–682.
(26) Kauffmann, E.; Frei, H.; Mathies, R. A. *Chem. Phys. Lett.* **1997**, *266*, 554–559.
(27) Dudek, R. C.; Weber, P. M. *J. Phys. Chem. A* **2001**, *105*, 4167–4171.
(28) Reid, P. J.; Doig, S. J.; Wickham, S. D.; Mathies, R. A. *J. Am. Chem. Soc.* **1993**, *115*, 4754–4763.
(29) Garavelli, M.; Page, C. S.; Celani, P.; Olivucci, M.; Schmid, W. E.; Trushin, S. A.; Fuss, W. *J. Phys. Chem. A* **2001**, *105*, 4458–4469.
(30) Geppert, D.; Seyfarth, L.; De Vivie-Riedle, R. *Appl. Phys. B: Lasers Opt.* **2004**, *79*, 987–992.
(31) Ruan, C.-Y.; Lobastov, V. A.; Srinivasan, R.; Goodson, B. M.; Ihee, H.; Zewail, A. H. *Proc. Natl. Acad. Sci. U.S.A.* **2001**, *98*, 7117–7122.
(32) Kurtz, L.; Hofmann, A.; de Vivie-Riedle, R. *J. Chem. Phys.* **2001**, *114*, 6151–6159.
(33) Jarmelo, S.; Reva, I. D.; Lapinski, L.; Nowak, M. J.; Fausto, R. *J. Phys. Chem. A* **2008**, *112*, 11178–11189.
(34) Frisch, M. J.; Trucks, G. W.; Schlegel, H. B.; Scuseria, G. E.; Robb, M. A.; Cheeseman, J. R.; Montgomery, J. A., Jr.; Vreven, T.; Kudin, K. N.; Burant, J. C.; Millam, J. M.; Iyengar, S. S.; Tomasi, J.; Barone, V.; Mennucci, B.; Cossi, M.; Scalmani, G.; Rega, N.; Petersson, G. A.; Nakatsuji, H.; Hada, M.; Ehara, M.; Toyota, K.; Fukuda, R.; Hasegawa, J.; Ishida, M.; Nakajima, T.; Honda, Y.; Kitao, O.; Nakai, H.; Klene, M.; Li, X.; Knox, J. E.; Hratchian, H. P.; Cross, J. B.; Bakken, V.; Adamo, C.; Jaramillo, J.; Gomperts, R.; Stratmann, R. E.; Yazyev, O.; Austin, A. J.; Cammi, R.; Pomelli, C.; Ochterski, J. W.; Ayala, P. Y.; Morokuma, K.; Voth, G. A.; Salvador, P.; Dannenberg, J. J.; Zakrzewski, V. G.; Dapprich, S.; Daniels, A. D.; Strain, M. C.; Farkas, O.; Malick, D. K.; Rabuck, A. D.; Raghavachari, K.; Foresman, J. B.; Ortiz, J. V.; Cui, Q.; Baboul, A. G.; Clifford, S.; Cioslowski, J.; Stefanov, B. B.; Liu, G.; Liashenko, A.; Piskorz, P.; Komaromi, I.; Martin, R. L.; Fox, D. J.; Keith, T.; Al-Laham, M. A.; Peng, C. Y.; Nanayakkara, A.; Challacombe, M.; Gill, P. M. W.; Johnson, B.; Chen, W.; Wong, M. W.; Gonzalez, C.; Pople, J. A. *Gaussian 03*, revision C.02; Gaussian, Inc.: Wallingford, CT, 2004.
(35) Lee, C.; Yang, W.; Parr, R. G. *Phys. Rev.* **1988**, *B37*, 785–789.
(36) Cossi, M.; Scalmani, G.; Rega, N.; Barone, V. *J. Chem. Phys.* **2002**, *117*, 43–54.
(37) Cossi, M.; Rega, N.; Scalmani, G.; Barone, V. *J. Comput. Chem.* **2003**, *24*, 669–681.
(38) Michalska, D.; Wysokinski, R. *Chem. Phys. Lett.* **2005**, *403*, 211–217.
(39) Michalska, D.; Zierkiewicz, W.; Bieńko, D. C.; Wojciechowski, W.; Zeegers-Huyskens, T. *J. Phys. Chem. A* **2001**, *105*, 8734–8739.
(40) Fogarasi, G.; Zhou, X.; Taylor, P. W.; Pulay, P. *J. Am. Chem. Soc.* **1992**, *114*, 8191–8201.
(41) Pulay, P.; Fogarasi, G.; Pang, F.; Boggs, J. E. *J. Am. Chem. Soc.* **1979**, *101*, 2550–2560.
(42) Martin, J. M. L.; Van Alsenoy, C. *Gar2ped*; University of Antwerp: Antwerp, Belgium, 1995.
(43) Danen, W. C.; Tipton, T. J.; Saunders, D. G. *J. Am. Chem. Soc.* **1971**, *93*, 5186–5189.
(44) Brouwer, A. M.; Jacobs, H. J. C. *Recl. Trav. Chim. Pays*−*Bas.* **1995**, *114*, 449–458.
(45) Rosado, M. T. S.; Lopes Jesus, A. J.; Reva, I. D.; Fausto, R.; Redinha, J. S. *J. Phys. Chem. A* **2009**, *113*, 7499–7507.
(46) Hofmann, A.; Kurtz, L.; de Vivie-Riedle, R. *Appl. Phys. B: Laser Opt.* **2000**, *71*, 391–396.
(47) Fuβ, W.; Schmid, W. E.; Trushin, S. A. *J. Chem. Phys.* **2000**, *112*, 8347–8362.
(48) Hofmann, A.; de Vivie-Riedle, R. *J. Chem. Phys.* **2000**, *112*, 5054–5059.
(49) Nakano, M.; Yamada, S.; Nagao, H.; Yamaguchi, K. *Int. J. Quantum Chem.* **1999**, *72*, 295–305.
(50) Lochbrunner, St.; Fuβ, W.; Schmid, W. E.; Kompa, K.-L. *J. Phys. Chem. A* **1998**, *102*, 9334–9344.
(51) Pullen, S. H.; Anderson, N. A.; Walker, L. A.; Sension, R. J. *J. Chem. Phys.* **1998**, *108*, 556–563.
(52) Pullen, S.; Walker, L. A.; Donovan, B.; Sension, R. J. *Chem. Phys. Lett.* **1995**, *242*, 415–420.
(53) Jacobs, H. J. C. *Pure Appl. Chem.* **1995**, *67*, 63–70.
(54) Olivucci, M.; Bernardi, F.; Ragazos, I.; Robb, M. A. *J. Am. Chem. Soc.* **1994**, *116*, 1077–1085.
(55) Reva, I. D.; Nowak, M. J.; Lapinski, L.; Fausto, R. *Chem. Phys. Lett.* **2006**, *429*, 382–388.
(56) Baldwin, J. E.; Krueger, S. M. *J. Am. Chem. Soc.* **1969**, *91*, 6444–6447.
(57) Woodward, R. B.; Hoffmann, R. *The Conservation of Orbital Symmetry*; Verlag Chemie: Weinheim, Germany, 1970.

JP100770V